PNAS RESEARCH ARTICLE | NEUROSCIENCE OPEN ACCESS

$K_v1.1$ preserves the neural stem cell pool and facilitates neuron maturation during adult hippocampal neurogenesis

Yuan-Hung Lin King[a,b,c,d], Chao Chen[b,c,d], John V. Lin King[a,b], Jeffrey Simms[e], Edward Glasscock[f], Shi-Bing Yang[g,h], Yuh-Nung Jan[b,c,d], and Lily Y. Jan[b,c,d,1]

Contributed by Lily Y. Jan; received October 4, 2021; accepted March 30, 2022; reviewed by Diane Papazian and Thomas Schwarz

Adult hippocampal neurogenesis is critical for learning and memory, and aberrant adult neurogenesis has been implicated in cognitive decline associated with aging and neurological diseases [J. T. Gonçalves, S. T. Schafer, F. H. Gage, *Cell* 167, 897–914 (2016)]. In previous studies, we observed that the delayed-rectifier voltage-gated potassium channel $K_v1.1$ controls the membrane potential of neural stem and progenitor cells and acts as a brake on neurogenesis during neonatal hippocampal development [S. M. Chou *et al.*, *eLife* 10, e58779 (2021)]. To assess the role of $K_v1.1$ in adult hippocampal neurogenesis, we developed an inducible conditional knockout mouse to specifically remove $K_v1.1$ from adult neural stem cells via tamoxifen administration. We determined that $K_v1.1$ deletion in adult neural stem cells causes overproliferation and depletion of radial glia-like neural stem cells, prevents proper adult-born granule cell maturation and integration into the dentate gyrus, and moderately impairs hippocampus-dependent contextual fear learning and memory. Taken together, these findings support a critical role for this voltage-gated ion channel in adult neurogenesis.

voltage-gated potassium channel | adult neurogenesis | hippocampus | learning and memory

Significance

Despite decades of research on adult neurogenesis, little is known about the role of bioelectric signaling in this process. In this study, we describe how a voltage-gated potassium channel, $K_v1.1$, supports adult neurogenesis by maintaining the neural stem cell niche and facilitating newborn neuron development. Additionally, we show that deletion of $K_v1.1$ from adult neural stem cells contributes to modest impairments in hippocampus-dependent contextual fear learning and memory. Dysfunctional adult neurogenesis has been implicated in cognitive decline associated with aging and neurological disease. Therefore, understanding the role of $K_v1.1$ in adult neurogenesis represents an opportunity to identify new therapeutic targets to promote healthy neurogenesis and cognition.

The subgranular zone of the hippocampus is one of two well-characterized neurogenic niches in the adult mouse brain. Integration of adult-born granule cells into the dentate gyrus is important for learning and memory, and impaired adult neurogenesis has been implicated in neurodegenerative and neuropsychiatric diseases (1–6). Adult hippocampal neurogenesis is divided into several developmental stages. Initially, quiescent neural stem cells with radial glia-like morphology—known as radial glia-like neural stem cells (type 1 cells)—activate and proliferate, either self-renewing or differentiating into intermediate neural progenitor cells with a glia-like phenotype (type 2a cells). As these cells differentiate, they lose their stem cell properties and display more neuron-like features (type 2b cells). Then, they develop into neuroblasts (type 3 cells) within a few days. Over the course of the next 2 wk to 4 wk, type 3 cells give rise to immature adult-born neurons that extend an apical dendrite into the dentate granule cell layer and grow secondary and tertiary dendrites. Simultaneously, they migrate from the subgranular zone into the dentate granule cell layer. Finally, adult-born granule cells mature into highly excitable neurons and integrate into the dentate gyrus circuitry (1–8).

While adult hippocampal neurogenesis is regulated by various environmental and endogenous factors, recent studies have also begun to explore the role of bioelectric signaling in this process. In nonexcitable cells, such as neural stem and progenitor cells, changes in the membrane potential can orchestrate proliferation, differentiation, migration, and survival during development (9). The membrane potential is controlled by ion channels, and ion channel dysfunction often results in neurodevelopmental disorders (10, 11). Interestingly, ion channels continue to modulate the membrane potential and cell dynamics of neural stem and progenitor cells during postnatal neurogenesis (12–19). In adult radial glia-like neural stem cells, gap junctions and inward rectifying potassium channels maintain the membrane potential (14, 17, 19). Their proliferation is also regulated by GABAergic and glutamatergic signaling, where these neurotransmitters activate their corresponding ligand-gated ion channels to alter the membrane potential (13, 15, 18). Additionally, local circuit activity is critical for young adult-born granule cells, which receive, in order, depolarizing GABAergic inputs, excitatory glutamatergic inputs, and, finally, inhibitory GABAergic inputs to advance through stages of maturation and survival (20–23).

In this study, we examine the role of the voltage-gated potassium channel $K_v1.1$ in adult hippocampal neurogenesis. $K_v1.1$ is encoded by the *Kcna1* gene in mice, and its expression begins increasing at ∼2 wk after birth and stabilizes in adulthood (24). $K_v1.1$ is well known for its role in regulating neuronal excitability and seizure activity (25, 26). Mice without functional $K_v1.1$—$K_v1.1$ null mutant mice and *megencephaly*

Author contributions: Y.-H.L.K., Y.-N.J., and L.Y.J. designed research; Y.-H.L.K., C.C., J.V.L.K., J.S., and S.-B.Y. performed research; E.G. contributed new reagents/analytic tools; Y.-H.L.K. analyzed data; and Y.-H.L.K. and L.Y.J. wrote the paper.

Reviewers: D.P., University of California, Los Angeles; and T.S., Harvard Medical School.

The authors declare no competing interest.

[1]To whom correspondence may be addressed. Email: lily.jan@ucsf.edu.

This article contains supporting information online at http://www.pnas.org/lookup/suppl/doi:10.1073/pnas.2118240119/-/DCSupplemental.

Published May 25, 2022.

(*mceph*) mice—not only develop seizures but also have an abnormally increased number of neurons in the dentate gyrus (12, 27–32). Using mosaic analysis with double markers (MADM) (33–35) in heterozygous *mceph* mice, we showed that $K_v1.1$ regulates neurogenesis in a cell-autonomous manner (32). We also found that loss of $K_v1.1$ function in $K_v1.1$ null mice depolarizes neonatal neural progenitor cells and increases proliferation through enhanced TrkB signaling (12). Because $K_v1.1$ null mice exhibit seizures beginning a few weeks after birth (27, 29–31), and seizure activity can affect neurogenesis (36, 37), it has not been feasible to assess the function of $K_v1.1$ in adult neurogenesis.

To address this issue and clarify the role of $K_v1.1$ in adult hippocampal neurogenesis, we created inducible $K_v1.1$ conditional knockout ($K_v1.1$ cKO) mice, which allowed us to specifically delete *Kcna1* from adult neural stem cells via tamoxifen injection and eliminate the confounding effect of seizures in our study. Using this mouse model, we first removed $K_v1.1$ in neonatal neural stem cells to validate our previous results with improved temporal resolution. Indeed, we recapitulated our previous observations showing that loss of $K_v1.1$ in neonatal neural stem cells increases proliferation and neuron production. Interestingly, the role of $K_v1.1$ in adult neural stem cells is more complex. We discovered that $K_v1.1$ prevents overproliferation and depletion of radial glia-like neural stem cells and enables proper adult-born granule cell maturation and positioning during adult neurogenesis. We further corroborated our findings of an age-dependent role of $K_v1.1$ using MADM of heterozygous $K_v1.1$ ($Kcna1^{+/-}$) mice (33–35). Finally, we determined that decreased adult neurogenesis in $K_v1.1$ cKO mice causes deficits in hippocampus-dependent contextual fear conditioning. These results demonstrate that $K_v1.1$ expression in adult neural stem cells is integral for preserving hippocampal neurogenesis and contextual learning and memory.

Results

Time-Controlled Deletion of $K_v1.1$ from Neural Stem Cells. To investigate the function of $K_v1.1$ in neural stem cells at various postnatal stages, we generated $K_v1.1$ cKO mice. We bred mice expressing a tamoxifen-inducible Cre recombinase (Cre) in neural stem cells (Nestin-Cre^{ERT2}) (38–40) with *Kcna1* floxed mice ($Kcna1^{fl/fl}$) (41) and Cre reporter mice (PC::G5-tdT) (42) to achieve temporal and cell type–specific control of *Kcna1* deletion. Upon tamoxifen injection, Cre begins expressing in neural stem cells, resulting in the removal of $K_v1.1$ and expression of tdTomato and GCaMP5G in the neural stem cells and their progeny. While the Cre-expressing neural stem cells are a small subset of all cell types in the dentate gyrus, the expression of tdTomato and GCaMP5G in these cells enables us to identify them for lineage tracing. We amplified the GCaMP5G signal with an anti-GFP antibody, because the anti-GFP antibody was compatible with our histology techniques using multiple cell markers. In this way, we successfully read out Cre expression in neural stem cells. To control for the possible effects of tamoxifen, Cre, and reporter expression on neural stem cell dynamics, we bred mice with wild-type *Kcna1* ($Kcna1^{+/+}$) with Nestin-Cre^{ERT2} and PC::G5-tdT mice for our control cohort ($K_v1.1$ WT) (*SI Appendix*, Fig. S1*A*).

To validate $K_v1.1$ knock-out after tamoxifen injection, we injected 8-wk-old $K_v1.1$ cKO and $K_v1.1$ WT mice with tamoxifen for three consecutive days and used fluorescence-activated cell sorting to isolate Cre-expressing tdTomato+ cells from the dentate gyrus at 2 wk post tamoxifen injection (*SI Appendix*, Fig. S1 *B–E*). We found that *Kcna1* messenger RNA expression was decreased by ∼90% in tdTomato+ cells in the dentate gyrus of $K_v1.1$ cKO mice compared to those of $K_v1.1$ WT mice ($P = 0.0001$) (*SI Appendix*, Fig. S1*F*). We also recorded the resting membrane potential of acutely dissociated tdTomato+ cells from the dentate gyrus at 2 wk post tamoxifen injection to determine whether $K_v1.1$ has been functionally deleted (*SI Appendix*, Fig. S2*A*). To assess the effect of acute $K_v1.1$ inhibition on resting membrane potential, we applied the selective $K_v1.1$ blocker, Dendrotoxin-K (DTx-K), to tdTomato+ $K_v1.1$ WT cells and observed a depolarized resting membrane potential (-70 ± 2.6 mV) compared to untreated $K_v1.1$ WT cells (-87 ± 0.58 mV) ($P = 0.0002$) (*SI Appendix*, Fig. S2 *B* and *C*). Consistent with our findings using DTx-K for acute $K_v1.1$ inhibition, we found that the resting membrane potential of tdTomato+ $K_v1.1$ cKO cells was similarly depolarized (-68 ± 1.0 mV) compared to $K_v1.1$ WT cells ($P = 0.0002$). Together, these results show that $K_v1.1$ is functionally knocked out of the Cre-expressing tdTomato+ neural stem cell lineage of $K_v1.1$ cKO mice by 2 wk post tamoxifen injection, likely resulting in depolarized cells.

Conditional Knockout of $K_v1.1$ in Neonatal Neural Stem Cells Increases Early Postnatal Hippocampal Neurogenesis. Both $K_v1.1$ null mice and *mceph* mutant mice display increased neonatal neurogenesis before seizure onset around 1 mo after birth (12, 27–32). As $K_v1.1$ cKO mice allowed us to examine the role of $K_v1.1$ in early postnatal neurogenesis with more precise temporal resolution, we focused on the role of $K_v1.1$ during peak hippocampal development at postnatal day 7 (P7), just before the second postnatal week when hippocampal neurogenesis begins transitioning from a more embryonic stage to adult stage (43, 44).

We injected tamoxifen at P0 to knock out $K_v1.1$ and conducted lineage tracing by injecting Bromodeoxyuridine (BrdU), which is incorporated into the DNA of actively dividing cells (45–48), at P7. We then quantified the number of progeny cells in the dentate gyrus of $K_v1.1$ cKO mice and $K_v1.1$ WT mice at P14 (*SI Appendix*, Fig. S3*A*). To determine which cell types were altered in the Cre-expressing GFP+ neural stem cell lineage, we costained the sections with established neural stem and progenitor cell marker, Sox2, and the postmitotic neuronal marker, NeuN. We found that neural stem and progenitor cell progenies from cells dividing at P7 (GFP+, BrdU+, Sox2+) in $K_v1.1$ cKO subgranular zone were increased by ∼60% ($P = 0.036$) (*SI Appendix*, Fig. S3 *B* and *C*). Within the dentate granule cell layer, neurons produced from cells dividing at P7 (GFP+, BrdU+, NeuN+) were increased by ∼55% ($P = 0.0007$) (*SI Appendix*, Fig. S3 *D* and *E*). The enhanced neonatal neurogenesis that we observed in $K_v1.1$ cKO mice is similar to our previous findings in $K_v1.1$ null mice (12), providing further evidence that $K_v1.1$ acts as a brake on early postnatal neurogenesis.

Deletion of $K_v1.1$ in Adult Neural Stem Cells Leads to a Transient Activation Followed by a Depletion of Radial Glia-Like Cells. Next, we investigated the role of $K_v1.1$ in adult hippocampal neurogenesis. To specifically ablate $K_v1.1$ in the adult neural stem cell lineage, we injected 8-wk-old adult mice with tamoxifen for three consecutive days. Unlike the $K_v1.1$ null mice and *mceph* mutant mice, adult $K_v1.1$ cKO mice injected with tamoxifen did not display seizure phenotypes, thereby allowing us to eliminate the confounding effects of seizures on adult neurogenesis from our study.

We started by examining mice 4 wk after tamoxifen injection to assess the early effects of $K_v1.1$ deletion on adult quiescent radial glia-like neural stem cells (type 1 cells), which are labeled by Sox2 and the glial marker, GFAP. As they become activated, radial glia-like neural stem cells begin expressing the mitotic marker, MCM2 (Fig. 1*A*) (49). At 4 wk post tamoxifen injection, quiescent (GFP+, GFAP+, Sox2+, MCM2−) and activated (GFP+, GFAP+, Sox2+, MCM2+) radial glia-like

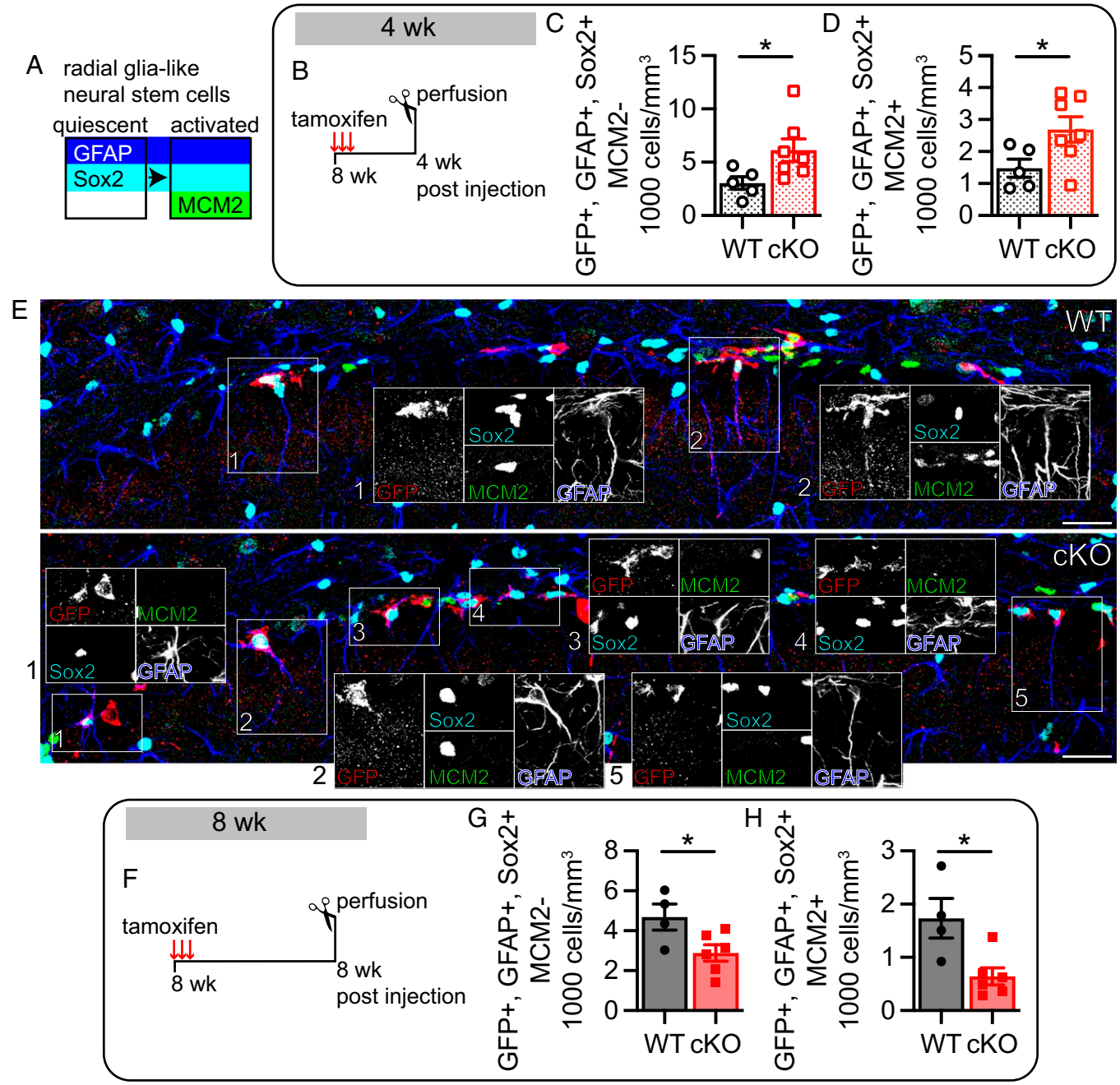

Fig. 1. Deletion of $K_v1.1$ in adult neural stem cells results in an initial increase of radial glia-like neural stem cells before eventual depletion of the radial glia-like neural stem cell pool. (*A*) Diagram of cell marker expression during neural stem cell development. Quiescent radial glia-like neural stem cells express GFAP and Sox2. As radial glia-like neural stem cells start proliferating, they express MCM2. (*B*) Protocol to assess short-term effects of $K_v1.1$ cKO on adult hippocampal neurogenesis. At 8 wk old, $K_v1.1$ cKO mice and $K_v1.1$ WT mice were injected with tamoxifen for three consecutive days to induce Cre expression and, in $K_v1.1$ cKO mice, *Kcna1* deletion. At 4 wk post tamoxifen injection, we carried out immunostaining of GFP+ radial glia-like neural stem cells. (*C* and *D*) Quantification (cells per cubic millimeter) of adult radial glia-like neural stem cells at 4 wk post tamoxifen injection. Quiescent radial glia-like neural stem cells (GFP+, GFAP+, Sox2+, MCM2−) ($P = 0.048$) and activated radial glia-like neural stem cells (GFP+, GFAP+, Sox2+, MCM2+) ($P = 0.046$) were increased in $K_v1.1$ cKO mice ($n = 7$) compared to $K_v1.1$ WT mice ($n = 5$). (*E*) Representative image showing expression of GFP (red), GFAP (blue), Sox2 (cyan), and MCM2 (green) in the ventral blade of the dentate gyrus in $K_v1.1$ WT mice (*Top*) and $K_v1.1$ cKO mice (*Bottom*). Within the $K_v1.1$ WT overlay, quiescent (2) and activated (1) radial glia-like neural stem cells are boxed; within the $K_v1.1$ cKO overlay, quiescent (1, 3 to 5) and activated (2) radial glia-like neural stem cells are boxed. Each individual channel of the boxed areas is displayed. (Scale bar, 25 μm.) (*F*) Protocol to assess long-term effects of $K_v1.1$ cKO on adult neurogenesis. $K_v1.1$ cKO mice and $K_v1.1$ WT mice were injected at 8 wk of age with tamoxifen for three consecutive days to induce Cre expression and *Kcna1* deletion. At 8 wk post tamoxifen injection, we carried out immunostaining of GFP+ radial glia-like neural stem cells. (*G* and *H*) Quantification (cells per cubic millimeter) of adult radial glia-like neural stem cells at 8 wk post tamoxifen injection. Quiescent radial glia-like neural stem cells (GFP+, GFAP+, Sox2+, MCM2−) ($P = 0.039$) and activated radial glia-like neural stem cells (GFP+, GFAP+, Sox2+, MCM2+) ($P = 0.016$) were decreased in $K_v1.1$ cKO mice ($n = 6$) compared to $K_v1.1$ WT mice ($n = 4$). (*C*, *D*, *G*, and *H*) Unpaired two-tailed Student's *t* test. $^*P < 0.05$. Data are presented as mean ± SEM.

neural stem cells were increased by ~100% ($P = 0.048$) and ~80% ($P = 0.046$), respectively, in $K_v1.1$ cKO mice as compared to $K_v1.1$ WT mice (Fig. 1 *B–E*). This suggests that loss of $K_v1.1$ initially promotes both radial glia-like neural stem cell division and self-renewal. Instead of self-renewing, radial glia-like neural stem cells can also divide and differentiate into type 2a cells, losing their GFAP expression (*SI Appendix*, Fig. S4*A*). To determine whether loss of $K_v1.1$ alters radial glia-like neural stem cell differentiation, we quantified the amount of type 2a cells (GFP+, GFAP−, Sox2+, MCM2+) and found a trend toward statistical significance that type 2a cells in $K_v1.1$ cKO mice were increased by ~70% at 4 wk post tamoxifen injection ($P = 0.068$) (*SI Appendix*, Fig. S4 *B* and *D*). It is possible that the trend toward an increase of type 2a cells arose from either enhanced radial glia-like neural stem cell proliferation, which pushed radial glia-like neural stem cells to both self-renew and differentiate, or increased proliferation of both radial glia-like neural stem cells and type 2a cells in $K_v1.1$ cKO mice. Interestingly, the increase in radial glia-like neural stem cells and type 2a cells did not lead to additional type 2b and proliferating type 3 cells (GFP+, GFAP−, Sox2−, MCM2+) (*SI Appendix*, Fig. S4 *C* and *D*). From these observations, $K_v1.1$ expression seems to discourage adult radial glia-like neural stem cell division.

To determine the long-term effects of $K_v1.1$ deletion, we investigated changes in the neural stem cell lineage at 8 wk after tamoxifen injection. Surprisingly, quiescent (GFP+, GFAP+, Sox2+, MCM2−) and activated (GFP+, GFAP+, Sox2+, MCM2+) radial glia-like neural stem cells were reduced by ~40% ($P = 0.039$) and ~65% ($P = 0.016$), respectively, in $K_v1.1$ cKO mice as compared to $K_v1.1$ WT mice (Fig. 1 *F–H*). We interpret this to mean that the initial increase in radial glia-like neural stem cell proliferation eventually exhausted their ability to self-renew and depleted the radial glia-like neural stem cell pool. We also examined the role of $K_v1.1$ in type 2a and proliferating type 2b/3 cells. Because of the variability of the type 2a (GFP+, GFAP−, Sox2+, MCM2+) cell counts, we were unable to determine, with confidence, whether they were altered in the $K_v1.1$ cKO mice at 8 wk post tamoxifen injection ($P = 0.14$) (*SI Appendix*, Fig. S4 *E* and *G*). We did not find a difference in type 2b/3 cells (GFP+, GFAP−, Sox2−, MCM2+) between $K_v1.1$ cKO mice and $K_v1.1$ WT mice at 8 wk post tamoxifen injection (*SI Appendix*, Fig. S4 *F* and *G*). Taken together, these results indicate that $K_v1.1$ acts as a brake on overproliferation to prevent early depletion of the neurogenic stem cell pool.

Eliminating $K_v1.1$ from Adult Neural Stem Cells Prevents Proper Adult-Born Granule Cell Maturation and Positioning. To investigate the role of $K_v1.1$ in later stages of adult-born granule cell production, we stained for a neurogenesis marker, doublecortin (DCX) at 8 wk post tamoxifen injection. DCX begins to express in a subset of type 2b cells and ceases to express as they become NeuN+ mature neurons (50–52). Interestingly, there was a ~55% decrease in GFP+, DCX+ cells ($P = 0.041$) (Fig. 2 *A* and *D*) in $K_v1.1$ cKO mice although the amount of proliferating type 2b/3 cells was not altered (*SI Appendix*, Fig. S4*F*). This raises the question whether the observed decrease in GFP+, DCX+ cells was due to the altered development of young adult-born granule cells. We relied on the distinct morphology of DCX+ cells at different stages of maturation to identify more-developed DCX+ adult-born granule cells as those with tertiary dendrites (50–52). Interestingly, in the $K_v1.1$ cKO lineage, there was a ~75% decrease in the number of GFP+, DCX+ cells with tertiary dendrites ($P = 0.012$) as well as a ~45% decrease in the proportion of more-developed GFP+, DCX+ cells with tertiary dendrites among all GFP+, DCX+ cells ($P = 0.017$) (Fig. 2 *B–D*). Together, these results indicate that loss of $K_v1.1$ hinders young adult-born granule cell maturation.

Those $K_v1.1$ cKO neurons that successfully matured were also more likely to be inappropriately positioned. As young adult-born granule cells mature, they migrate from the subgranular zone into the dentate granule cell layer such that a majority are positioned within the inner two-thirds of the dentate granule cell layer (Fig. 2*E*) (20, 53). The percentage of mature GFP+ adult-born granule cells (GFP+, NeuN+) found in the outer third of the dentate granule cell layer at 8 wk post tamoxifen injection in $K_v1.1$ cKO mice was ~215% higher than that of $K_v1.1$ WT mice ($P = 0.033$) (Fig. 2 *F* and *H*), indicating that loss of $K_v1.1$ impairs adult-born granule cell positioning. These findings point toward a critical role of $K_v1.1$ in facilitating successful adult-born granule cell development, as aberrant migration and positioning of adult-born granule cells has been found in mouse models of traumatic brain injury, schizophrenia, and neurodegeneration (54–56). These findings may also explain why we observed a ~50% reduction in mature GFP+ adult-born granule cells (GFP+, NeuN+) in $K_v1.1$ cKO mice by 8 wk post tamoxifen injection ($P = 0.020$) (Fig. 2 *G* and *H*). As young adult-born granule cells from neural stem cells lacking $K_v1.1$ cannot properly mature and position themselves, they are likely unable to successfully integrate into the dentate gyrus circuitry. Taken together, our observations indicate that $K_v1.1$ is integral for adult-born granule cells to develop proper morphology and positioning, which would allow them to incorporate synaptic inputs, integrate into the hippocampal circuitry, and fulfill their critical functions in learning and memory.

MADM Analyses Reveal a Transient Increase of Neural Stem Cell Lineage Lacking $K_v1.1$. In our previous studies, we performed MADM (33–35) with heterozygous $K_v1.1$ (*Kcna1*$^{+/-}$) mice, in which sparse somatic recombination driven by constitutively active Nestin-Cre generates a subpopulation of neural stem cells that lack $K_v1.1$ (Nestin-Cre;*Kcna1*$^{+/-}$;MADM-6) (Fig. 3*A*) (12). Homozygous $K_v1.1$ null neural stem cell lineages are marked with GFP, and homozygous $K_v1.1$ wild-type neural stem cell lineages are marked with tdTomato. Using this model, we observed ~180% increase in progeny neurons from $K_v1.1$ null neural stem cells in the dentate granule cell layer of 2- to 3-mo-old Nestin-Cre;*Kcna1*$^{+/-}$;MADM-6 mice ($P < 0.0001$) [Fig. 3 *B* and *C*; data from 1-mo-old and 2- to 3-mo-old cohorts originally published in figure 1 of Chou et al. (12)]. This is consistent with our findings from $K_v1.1$ null mice and $K_v1.1$ cKO mice that loss of $K_v1.1$ in neonatal neural stem cells promotes neonatal radial glia-like neural stem cell proliferation and neuronal production (*SI Appendix*, Fig. S3) (12). In 2- to 3-mo-old Nestin-Cre;*Kcna1*$^{+/-}$;MADM-6 mice, presumably, a large population of neonatal-born neurons remains, as neonatal-born neurons begin apoptosis ~2 mo after birth (57–59). However, once the mice have reached 6 mo to 13 mo of age, neonatal-born $K_v1.1$ null progeny neurons would have been trimmed via apoptosis and therefore appear as a smaller portion of the GFP+ population. Indeed, we found no increase in $K_v1.1$ null progeny neurons in the dentate granule cell layer of 6- to 13-mo-old mice (Fig. 3 *B* and *C*). As the loss of $K_v1.1$ negatively impacts adult neurogenesis (Fig. 2), we conclude that adult-born $K_v1.1$ null progeny neurons are unable to adequately replenish the GFP+ population. Thus, the transient increase of $K_v1.1$ null progeny neurons in the MADM mice heterozygous for $K_v1.1$ null

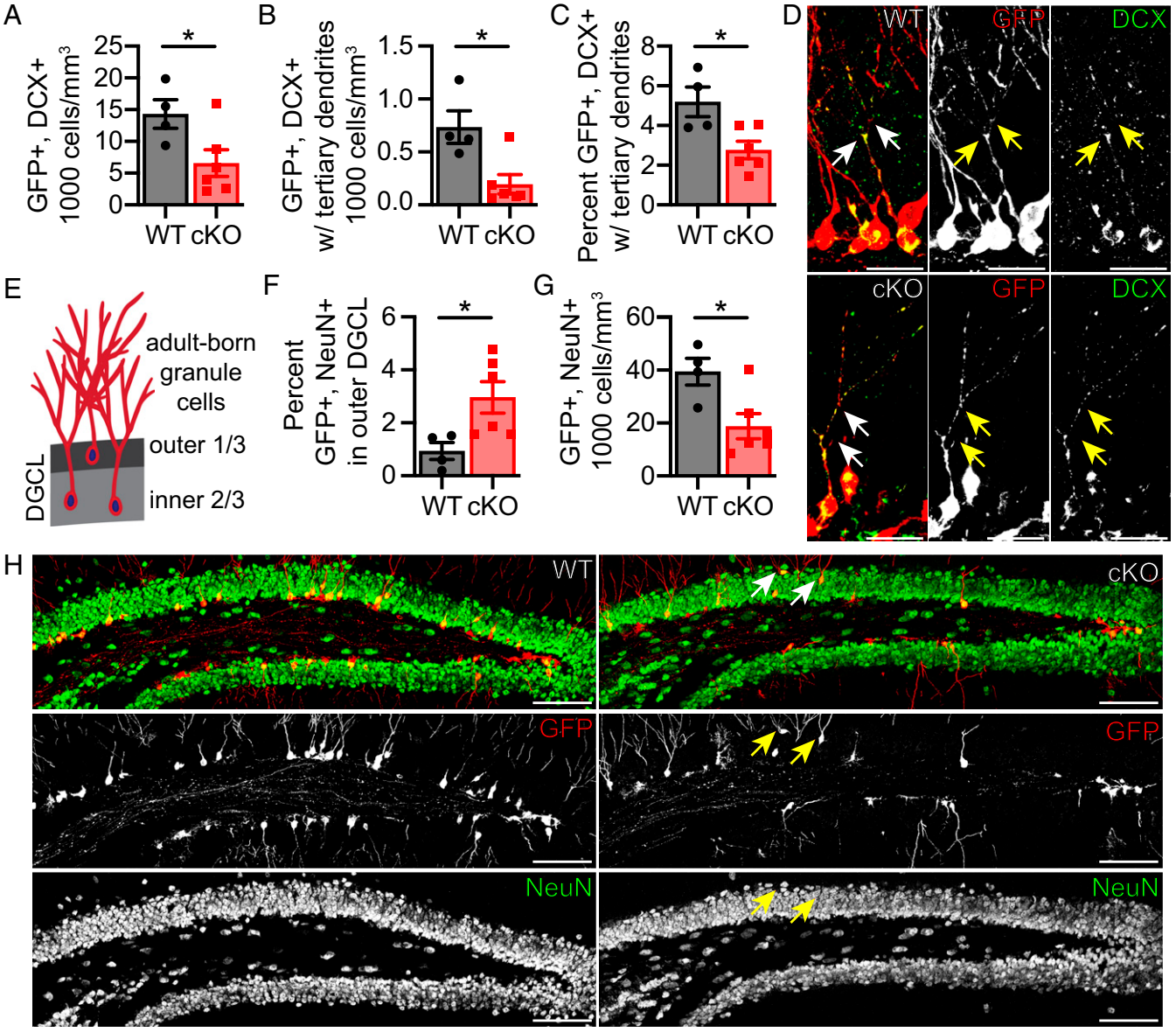

Fig. 2. Loss of $K_v1.1$ impairs adult hippocampal neurogenesis by altering doublecortin-expressing (DCX+) cell maturation and adult-born granule cell positioning. (*A*) Quantification (cells per cubic millimeter) of GFP+, DCX+ cells. Fewer GFP+, DCX+ cells were found in $K_v1.1$ cKO mice ($n = 6$) compared to $K_v1.1$ WT mice ($n = 4$) ($P = 0.041$). (*B*) Quantification (cells per cubic millimeter) of more-mature GFP+, DCX+ cells with tertiary dendrites. A decrease in GFP+, DCX+ cells with tertiary dendrites in $K_v1.1$ cKO mice compared to $K_v1.1$ WT mice was observed ($P = 0.012$). (*C*) Percentage of GFP+, DCX+ cells that display more-mature tertiary dendrite morphology was reduced in $K_v1.1$ cKO mice compared to $K_v1.1$ WT mice ($P = 0.017$). (*D*) Representative image of merged and individual signals of GFP (red) and DCX (green) in the dentate gyrus of $K_v1.1$ WT mice (*Top*) and $K_v1.1$ cKO mice (*Bottom*). Branching of DCX+ cells with tertiary dendrites is marked (arrows). (Scale bar, 25 μm.) (*E*) Cartoon of adult-born granule cell development. Adult-born granule cells migrate away from the subgranular zone toward the molecular layer and usually position themselves within the inner two-thirds of the dentate granule cell layer (DGCL). (*F*) Percentage of GFP+, NeuN+ cells in outer layer of the DGCL was diminished in $K_v1.1$ cKO mice compared to $K_v1.1$ WT mice ($P = 0.033$). (*G*) Quantification (cells per cubic millimeter) of GFP+, NeuN+ cells. GFP+, NeuN+ cells were decreased in $K_v1.1$ cKO mice compared to $K_v1.1$ WT mice ($P = 0.020$). (*H*) Representative image of overlayed and individual GFP (red) and NeuN (green) signals of the dentate gyrus from $K_v1.1$ WT mice (*Left*) and $K_v1.1$ cKO mice (*Right*) are shown. GFP+, NeuN+ cells in the outer third of the dentate granule cell layer are marked (arrows). (Scale bar, 100 μm.) (*A*, *B*, *C*, *F*, and *G*) Unpaired two-tailed Student's *t* test; $*P < 0.05$. Data are presented as mean ± SEM.

mutation supports the hypothesis that $K_v1.1$ plays an age-dependent role in adult neurogenesis.

Mice with Conditional Knockout of $K_v1.1$ from Adult Neural Stem Cells Display Impairments in Contextual Fear Conditioning. The hippocampus is important for contextual learning and memory; decreased hippocampal neurogenesis has been found to impair contextual fear conditioning, where mice learn to associate an environment with fear (60–63), and pattern separation, where they learn to discriminate between two similar contexts (40, 64, 65). Since the deletion of $K_v1.1$ in adult neural stem cells reduced adult hippocampal neurogenesis (Fig. 2), we hypothesized that $K_v1.1$ cKO mice would have learning and memory deficits compared to $K_v1.1$ WT mice. We conducted behavioral tests on $K_v1.1$ cKO mice starting at ∼4 mo of age when adult neurogenesis is less variable than at 2 mo of age (66). We injected ∼4-mo-old $K_v1.1$ cKO mice with tamoxifen for five consecutive days to induce Cre expression and $K_v1.1$ deletion in more neural stem cells (Fig. 4*A*). In control behavioral experiments, we did not find statistically significant differences between $K_v1.1$ cKO and $K_v1.1$ WT mice in the elevated plus maze, open field, and hotplate test (*SI Appendix*, Fig. S5). These results indicate that the mobility, anxiety, and pain perception of $K_v1.1$ cKO mice are not different from those of

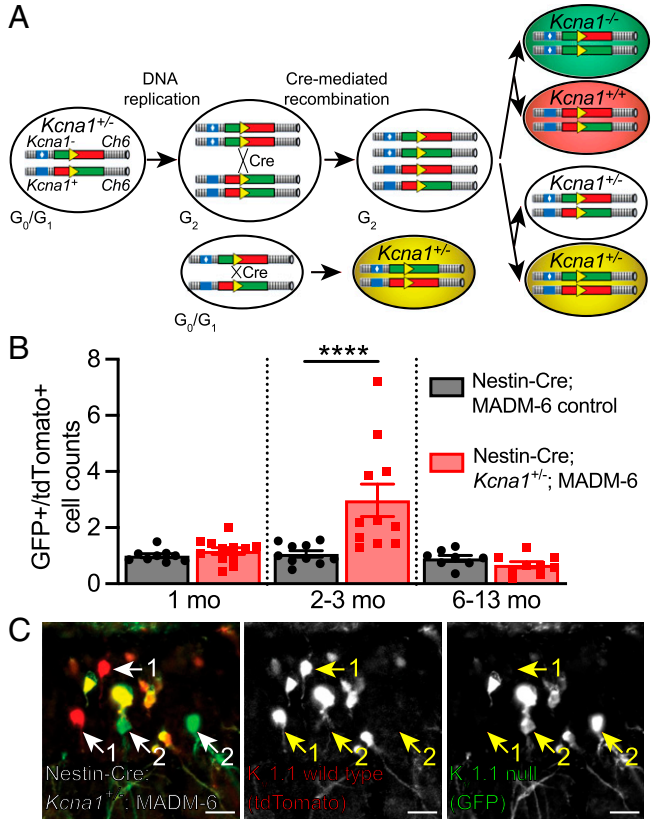

Fig. 3. MADM analysis reveals a transient increase in $K_v1.1$ null progeny cells in the dentate gyrus of 2- to 3-mo-old mice. (*A*) Schematic of MADM method (33–35) for generating $K_v1.1$ null (GFP+) and $K_v1.1$ wild-type (tdTomato+) progeny. MADM-6 marker mice were bred to *Kcna1*$^{+/-}$ mice and Nestin-Cre mice. At G_2 phase of the cell cycle, Cre induces infrequent interchromosomal recombination and restores functional GFP and tdTomato genes. During chromosome segregation, equal numbers of either *Kcna1*$^{-/-}$ (GFP+) and *Kcna1*$^{+/+}$ (tdTomato+) progenies or colorless *Kcna1*$^{+/-}$ and dual-color *Kcna1*$^{+/-}$ (yellow) progenies are generated. Dual-color *Kcna1*$^{+/-}$ (yellow) progenies can also be generated by interchromosomal recombination at G_0/G_1 phase of the cell cycle (*Below*). (*B*) Ratio of GFP+ to tdTomato+ cells in Nestin-Cre;*Kcna1*$^{+/-}$;MADM-6 and Nestin-Cre;MADM-6 control mice at 1 mo old, 2 mo to 3 mo old, and 6 mo to 13 mo old. The ratio of $K_v1.1$ null (GFP+) to $K_v1.1$ wild-type (tdTomato+) progeny cells was increased in 2- to 3-mo-old Nestin-Cre;*Kcna1*$^{+/-}$;MADM-6 mice compared to Nestin-Cre;MADM-6 control mice ($P < 0.0001$). There was no difference in the ratio of $K_v1.1$ null (GFP+) to $K_v1.1$ wild-type (tdTomato+) progeny cells between the two genotypes at 1 mo old and 6 mo to 13 mo old. Two-way ANOVA followed by Sidak's multiple comparisons test: genotype effect ($F_{1,\ 53} = 7.0$, $P = 0.011$), age effect ($F_{2,\ 53} = 10$, $P = 0.0002$), and genotype × age interaction ($F_{2,\ 53} = 8.2$, $P = 0.0008$); Sidak's multiple comparisons: 1 mo old ($P = 0.96$), 2 mo to 3 mo old ($P < 0.0001$), and 6 mo to 13 mo old ($P = 0.93$). Nestin-Cre;*Kcna1*$^{+/-}$;MADM-6: 1 mo old ($n = 12$); 2 mo to 3 mo old ($n = 11$); 6 mo to 13 mo old ($n = 9$). Nestin-Cre;MADM-6 control: 1 mo old ($n = 9$); 2 mo to 3 mo old ($n = 10$); 6 mo to 13 mo old ($n = 8$). (*C*) Representative image with overlay and individual signals displaying $K_v1.1$ null progenies (GFP+, green), $K_v1.1$ wild-type progenies (tdTomato+, red), and $K_v1.1$ heterozygous (GFP+ and tdTomato+, yellow) from the dentate gyrus of 8-mo-old Nestin-Cre;*Kcna1*$^{+/-}$;MADM-6 mice. $K_v1.1$ wild-type (1) and $K_v1.1$ null (2) cells are marked (arrows). (Scale bar, 25 μm.) ****$P < 0.0001$. Data are presented as mean ± SEM. Data from 1-mo-old and 2- to 3-mo-old cohorts were originally published in figure 1 of Chou et al. (12).

$K_v1.1$ WT mice. To test for the effects of $K_v1.1$ cKO on hippocampus-dependent learning and memory, we used a protocol with three segments to first examine contextual fear conditioning, then contextual recall and generalization, and, finally, contextual discrimination (pattern separation) (64, 67).

First, mice underwent 3 d of contextual fear conditioning where they learned to associate the fear context with a foot shock. On days 1 to 3, they were placed in the fear context, a single foot shock was administered 3 min into the session, and mice were removed 1 min after the shock. Percent freezing before (0 min to 3 min) and after (3 min to 4 min) the foot shock was measured daily (Fig. 4*B*). The two genotypes did not display differences in percent freezing before the foot shock on day 1, showing that they have similar freezing levels at baseline (Fig. 4*C*). Interestingly, we found that $K_v1.1$ cKO mice appeared to have reduced expression of contextual fear memory (genotype effect [$F_{1,\ 33} = 7.5$, $P = 0.010$], day effect [$F_{1.8,\ 61} = 197$, $P < 0.0001$], and genotype × day interaction [$F_{2,\ 66} = 2.9$, $P = 0.060$]), which manifested as a ∼25% and ∼20% reduction in freezing time prior to foot shock as compared to $K_v1.1$ WT on day 2 and day 3 (post hoc analysis of linear mixed-model using Sidak's multiple comparisons test: day 2 [$P = 0.10$], and day 3 [$P = 0.010$]) (Fig. 4*C*). Given that there was no difference between the two genotypes in percent freezing following the shock on days 1 to 3 (Fig. 4*D*), this study indicates that $K_v1.1$ cKO mice exhibited a mild deficit in contextual fear conditioning.

Next, we demonstrated that both genotypes generalized their learned fear to a similar novel neutral context (*SI Appendix*, Fig. S6 *A–C*), thus allowing us to proceed to the third segment of our experiment and assess their ability to discriminate between the two contexts. In the pattern separation task on days 6 to 19, mice were placed in the two contexts daily, and shock was again administered in the fear context. Percent freezing was averaged for each 2-d block, to reduce variability (*SI Appendix*, Fig. S6*D*). As the mice learned to discriminate between the two contexts, they froze more in the fear context than the neutral context. We found no significant genotype effect in the pattern separation test (*SI Appendix*, Fig. S6 *E–I*).

To validate that the modest effect on contextual fear conditioning we observed was due to decreased adult hippocampal neurogenesis in $K_v1.1$ cKO mice, we collected brain tissues from the behavioral cohorts and stained for NeuN to assess the extent of neurogenesis in the GFP+ lineages with tamoxifen-induced Cre expression and, in $K_v1.1$ cKO cohort, deletion. We found that adult neurogenesis was decreased by ∼20% in $K_v1.1$ cKO mice as compared to $K_v1.1$ WT controls ($P = 0.037$) (Fig. 4*E*). These observations are consistent with previous studies reporting diminished adult neurogenesis resulting in deficient contextual fear conditioning (60–63). Whereas past studies using X-ray irradiation to reduce adult neurogenesis by more than ∼90% have produced deficits in pattern separation (40, 64), the ∼20% decrease in adult neurogenesis caused by the loss of $K_v1.1$ is probably insufficient to impair their performance in the pattern separation test. In summary, these results indicate that deletion of $K_v1.1$ hinders adult neurogenesis, resulting in mild impairments in contextual fear conditioning.

Discussion

Adult hippocampal neurogenesis is critical for learning and memory, and altered adult neurogenesis has been implicated in aging and neurological disorders (1–6). Although voltage-gated ion channels have been shown to modulate the membrane potential and cell dynamics of neural stem and progenitor cells during vertebrate and invertebrate neurodevelopment (9–11, 68–70), the role of bioelectric signaling in adult hippocampal neurogenesis has only recently begun to be explored. In our previous study, we found that genetic ablation of $K_v1.1$ depolarizes neonatal neural progenitor cells and increases their proliferation through enhanced TrkB signaling in neonatal hippocampal development (12). As $K_v1.1$ null mice develop seizures that could impact adult neurogenesis (27, 29–31, 36, 37)

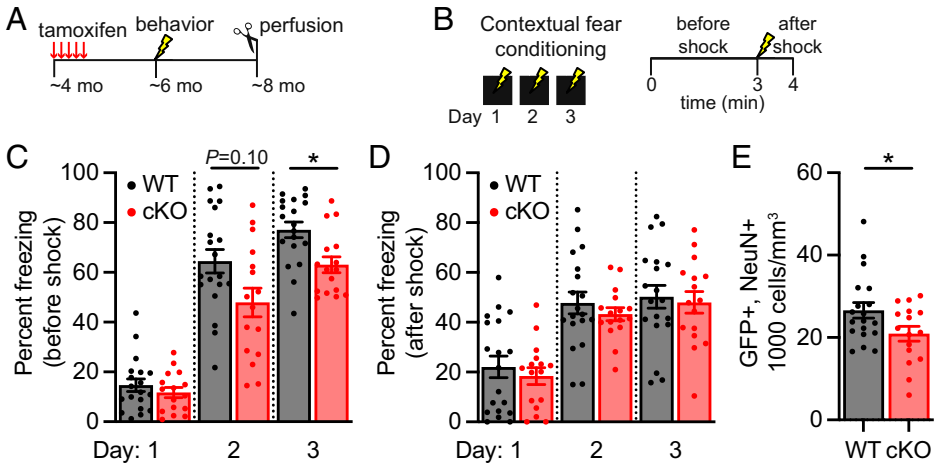

Fig. 4. $K_v1.1$ cKO mice display impairments in contextual fear conditioning. (*A*) Behavioral paradigm for assessing learning and memory in $K_v1.1$ cKO mice and $K_v1.1$ WT mice. Tamoxifen was injected for five consecutive days in ~4-mo-old mice. Contextual fear conditioning started at ~6.5 wk post tamoxifen injection. Mice were perfused at ~8 mo of age. (*B*) Protocol for contextual fear conditioning. On days 1 to 3, the mice were shocked in the fear context. Percent freezing before the shock (0 min to 3 min) and after the shock (3 min to 4 min) were measured. (*C*) Quantification of percent freezing before shock on days 1 to 3, revealing a modest impairment of contextual fear learning and memory in $K_v1.1$ cKO mice ($n = 16$) compared to $K_v1.1$ WT mice ($n = 19$). Linear mixed model with REML and Geisser–Greenhouse correction followed by Sidak's multiple comparisons test on days 1 to 3: genotype effect ($F_{1, 33} = 7.5$, $P = 0.010$), day effect ($F_{1.8, 61} = 197$, $P < 0.0001$), and genotype × day interaction ($F_{2, 66} = 2.9$, $P = 0.060$); Sidak's multiple comparisons: day 1 ($P = 0.75$), day 2 ($P = 0.098$), and day 3 ($P = 0.010$). (*D*) Quantification of percent freezing after shock on days 1 to 3, revealing no difference between $K_v1.1$ cKO mice and $K_v1.1$ WT mice. Linear mixed model with REML and Geisser–Greenhouse correction followed by Sidak's multiple comparisons test on days 1 to 3: genotype effect ($F_{1, 33} = 0.54$, $P = 0.47$), day effect ($F_{1.7, 55} = 59$, $P < 0.0001$), and genotype × day interaction ($F_{2, 66} = 0.077$, $P = 0.93$); Sidak's multiple comparisons: day 1 ($P = 0.88$), day 2 ($P = 0.77$), and day 3 ($P = 0.98$). (*E*) Quantification (cells per cubic millimeter) of GFP+, NeuN+ cells to assess the amount of adult-born granule cells in the dentate gyrus of $K_v1.1$ cKO and $K_v1.1$ WT behavioral cohorts. Neurogenesis was decreased in $K_v1.1$ cKO mice compared to $K_v1.1$ WT mice ($P = 0.037$). Unpaired two-tailed Student's *t* test with Welch's correction. $P < 0.10$ indicated; $^*P < 0.05$. Data are presented as mean ± SEM.

and confound the possible impact of $K_v1.1$ deletion on adult neurogenesis, we developed a strategy for inducible conditional knockout of $K_v1.1$ from neural stem cells of adult mice (*SI Appendix*, Fig. S1*A*). These $K_v1.1$ cKO mice allowed us to examine the role of $K_v1.1$ at different stages of adult neurogenesis and better elucidate the role of $K_v1.1$ during neonatal and adult development.

During early steps of adult hippocampal neurogenesis, $K_v1.1$ is important for preserving the radial glia-like neural stem cell (type 1 cell) pool (Fig. 5*A*), which is maintained by a delicate balance between radial glia-like neural stem cell quiescence and activation (71). Initially, radial glia-like neural stem cells without $K_v1.1$ rapidly divide to 1) self-renew, generating more quiescent radial glia-like neural stem cells (Fig. 1*C*), and 2) differentiate, likely producing more type 2a cells (*SI Appendix*, Fig. S4*B*). However, radial glia-like neural stem cells have varying self-renewal capacity. Over time, increased proliferation in the absence of $K_v1.1$ may become unsustainable and might exhaust the radial glia-like neural stem cells with limited proliferative potential as they undergo terminal differentiation and are eliminated from the progenitor pool (72, 73). Interestingly, the switch between radial glia-like neural stem cell quiescence and activation can be regulated by network activity of glutamatergic mossy cells and long-range GABAergic neurons. Ablation of both cell types can produce a similar initial activation followed by depletion of radial glia-like neural stem cells (13, 15, 18). In addition to regulation via synaptic inputs, our study suggests that radial glia-like neural stem cells may rely on $K_v1.1$ channel activity to prevent their subsequent activation and depletion (*SI Appendix*, Fig. S2 and Fig. 1). Perhaps loss of $K_v1.1$ depolarizes adult neural stem and progenitor cells and promotes proliferation through increased TrkB signaling, as we previously observed in neonatal neurogenesis (12).

Our study further reveals that loss of $K_v1.1$ in the neural stem cell lineage impedes adult-born granule cell development in later stages of adult neurogenesis. In $K_v1.1$ cKO mice, there was a reduction of DCX-expressing cells as well as impairment of adult-born granule cell maturation and positioning (Fig. 2 *A*–*F*). Notably, aberrant positioning of adult-born granule cells has been observed in mouse models of traumatic brain injury, schizophrenia, and neurodegeneration (54–56). Failing to properly mature and position themselves, young adult-born granule cells produced from neural stem cells lacking $K_v1.1$ likely struggle to integrate into the dentate gyrus circuit, resulting in decreased survival of new adult-born granule cells and reduced mature adult-born granule cells (NeuN+) in $K_v1.1$ cKO mice (Fig. 2 *G* and *H*). Interestingly, a recent study discovered that postmortem samples from patients with neurodegenerative disease display a similar increase in radial glia-like neural stem cells and impairment in adult-born granule cell maturation and positioning (74). In mouse models, failures in adult neurogenesis often lead to deficits in hippocampus-dependent learning and memory (38, 40, 60–65). Indeed, $K_v1.1$ cKO mice have moderately diminished contextual fear learning and memory (Fig. 4). Together, these results underscore the critical function of $K_v1.1$ in maintaining adult-born granule cell maturation and positioning for proper integration into the dentate gyrus circuit and preservation of hippocampus-dependent learning and memory (Fig. 5*B*).

Our understanding of the role of $K_v1.1$ in adult neurogenesis also helps to clarify the role of $K_v1.1$ in neonatal neurogenesis. Given that we observed an initial increase in radial glia-like neural stem cell proliferation when $K_v1.1$ was removed from adult neural stem cells, the increase in neonatal neurogenesis observed when $K_v1.1$ is removed from neonatal neural stem cells in both $K_v1.1$ null mice (12) and $K_v1.1$ cKO mice (*SI Appendix*, Fig. S3) is likely to have arisen from neonatal radial glia-like neural stem cell overproliferation. Unlike adult neural stem and progenitor cells, neonatal neural stem and progenitor cells have extensive proliferative potential (43, 44) and produce neurons with delayed cell death (57–59). These properties of neonatal neurogenesis allow the neuronal progenies to last for a longer period, which would account for the initial increase in $K_v1.1$ null progeny of

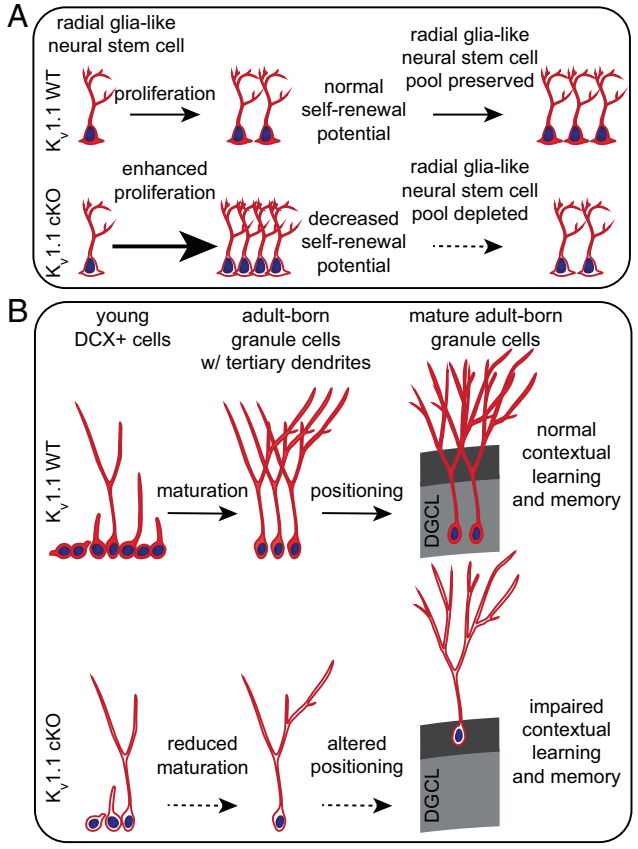

Fig. 5. Model of impaired adult hippocampal neurogenesis in K_v1.1 cKO mice with tamoxifen-induced Cre expression and K_v1.1 removal from neural stem cells. (*A*) During early stages of adult hippocampal neurogenesis, removal of K_v1.1 from neural stem cells enhances radial glia-like neural stem cell proliferation, leading to an initial increase of radial glia-like neural stem cells at 4 wk post tamoxifen injection (*Center*). Overproliferation diminishes the radial glia-like neural stem cells' self-renewal potential and depletes radial glia-like neural stem cells in K_v1.1 cKO mice, resulting in decreased radial glia-like neural stem cells by 8 wk post tamoxifen injection (*Right*). (*B*) In later stages of neurogenesis, K_v1.1 cKO mice have fewer DCX+ cells (*Left*), and these DCX+ cells have deficits in development with a reduction in the percentage and amount of adult-born granule cells with tertiary dendrites (*Center*). Fewer mature adult-born granule cells are produced in K_v1.1 cKO mice, and these adult-born granule cells are more likely to be mispositioned in the outer third of the DGCL (*Right*). Thus, K_v1.1 plays an important role in proper adult-born granule cell maturation and integration into the DGCL and in preserving hippocampus-dependent contextual learning and memory.

2- to 3-mo-old Nestin-Cre;*Kcna1*$^{+/-}$;MADM-6 mice (Fig. 3) before neuron death starting at 2 mo postmitosis (57–59). As the MADM mice age, neonatal-born K_v1.1 null neurons begin cell death, and radial glia-like neural stem cells lacking K_v1.1 become depleted, as in the case of adult K_v1.1 cKO mice. Together, these factors contribute to the transient increase of K_v1.1 null progeny neurons in 2- to 3-mo-old but not 6- to 13-mo-old Nestin-Cre;*Kcna1*$^{+/-}$;MADM-6 mice (Fig. 3). These results support our model that K_v1.1 functions to maintain hippocampal neurogenesis at multiple developmental timepoints.

In summary, we demonstrate that K_v1.1 is important for adult hippocampal neurogenesis and hippocampus-dependent contextual learning and memory. K_v1.1 likely regulates the neurogenic niche by preventing the overproliferation and depletion of radial glia-like neural stem cells. As young adult-born granule cells develop, loss of K_v1.1 impedes their dendritic maturation and positioning, likely hampering their integration into the circuit. These developmental failures in K_v1.1 cKO mice contribute to decreased adult-born granule cells and mild deficits in contextual fear learning and memory (Fig. 5). Our findings provide the basis for future studies to elucidate the impact of K_v1.1 regulation on adult neurogenesis under normal and pathophysiological conditions.

Materials and Methods

Animals. All experiments were approved by the Institutional Animal Care and Use Committees of the University of California, San Francisco and Academia Sinica. Two to five mice per cage were maintained in a temperature-controlled environment on a 12-h light/dark cycle with ad libitum access to food and water.

Kcna1$^{fl/fl}$ mice (41) were obtained from E.G.'s laboratory at Southern Methodist University, Dallas, TX. Nestin-Cre^{ERT2} mice (38–40) were obtained from Mazen Kheirbek's laboratory at University of California, San Francisco, CA. PC::G5-tdT mice (42) were obtained from the Jackson Laboratory. We utilized the PC::G5-tdT reporter line because its Cre reporter alleles are located on a different chromosome (Chr 11) from *Kcna1* (Chr 6). These three lines were bred together to create K_v1.1 cKO mice and maintained on a C57BL/6 background.

To create the Nestin-Cre;*Kcna1*$^{+/-}$;MADM-6 mice, the lines bred together were *Kcna1*$^{-/-}$ mice (31), obtained from Bruce Tempel's laboratory at the University of Washington, Seattle, WA; Nestin-Cre (Tg(Nes-cre)1Kln) (75), obtained from the Jackson Laboratory; and MADM-6 mice with *Rosa26*^{GT} (*Gt(ROSA)26Sor*$^{tm6(ACTB-EGFP*,-tdTomato)}$) and *Rosa26*^{TG} (*Gt(ROSA)26Sor*$^{tm7(ACTB-EGFP*)}$) (76), obtained from Liqun Luo's laboratory at Stanford University, Palo Alto, CA. All these mice were maintained on an ICR background. MADM experiments were performed as previously described (12).

Drug Administration. For neonatal tamoxifen (MilliporeSigma) administration, tamoxifen was dissolved in 100% corn oil (MilliporeSigma) at 10 mg of tamoxifen per mL. At P0, pups were injected once subcutaneously with 30 μL of 10 mg of tamoxifen per mL. For adult tamoxifen administration, tamoxifen was dissolved in a solution of 10% ethanol (200 proof, VWR) in corn oil at 20 mg of tamoxifen per mL. Adult 8-wk-old mice were intraperitoneally injected with 100 mg of tamoxifen per kg of body weight once per day for three consecutive days for single-cell suspension and immunohistochemistry. Adult ∼4-mo-old mice were injected with 100 mg of tamoxifen per kg of body weight once per day for five consecutive days for behavioral experiments. BrdU (MilliporeSigma) was dissolved in sterile normal (0.9%) saline at 5 mg of BrdU per mL. One dose of 50 mg of BrdU per kg of body weight was injected subcutaneously at P7.

Single-Cell Suspension for qPCR and Electrophysiology. At 2 wk post tamoxifen injection, mice were euthanized, and their brains were transferred into ice-cold 1× Hanks' balanced salt solution (HBSS). Under a dissecting microscope, dentate gyri were isolated and pooled from four mice of the same genotype. The Neural Tissue Dissociation (P) Kit (Miltenyi Biotec) was used to dissociate tissue into single cells. After a final HBSS wash, the cell pellet was resuspended in 800 μL of Hibernate A Low Fluorescence medium (BrainBits). Detailed methods for qPCR and electrophysiology are included in *SI Appendix, SI Materials and Methods*.

Immunostaining. Mice were anesthetized with isoflurane (Henry Schein Animal Health) before transcardial perfusion with cold phosphate-buffered saline (PBS) followed by cold 4% paraformaldehyde (PFA) in PBS. Brains were removed, postfixed overnight in 4% PFA for ∼24 h at 4 °C, washed in PBS, and immersed in 30% sucrose in PBS for a minimum of 48 h at 4 °C for cryoprotection. Then, the brains were frozen in optimal cutting temperature compound (Fisher Scientific). Free-floating 30-μm sagittal sections were collected from the lineage tracing cohort and coronal sections were collected from the behavior cohort into PBS using a cryostat (Lecia CM3050 S, Leica Microsystems). Afterward, the sections were transferred into cryoprotectant (30% ethylene glycol, 30% glycerol, 40% PBS) and stored at −20 °C.

For immunohistochemistry, sections were removed from the cryoprotectant, washed 3 × 10 min in PBS, treated with 15 min of 0.5% triton in PBS, and transferred into blocking buffer (5% normal donkey serum, 1% bovine serum albumin, 0.05% triton in PBS) for 1 h at room temperature. Then, they were incubated in primary antibodies overnight at 4 °C. The next day, they were washed 3 × 10 min with 0.05% triton in PBS and incubated in secondary antibodies for 1 h at room temperature. After 3 × 10 min PBS washes, they were mounted using Fluoromount G mounting media with DAPI (Southern Biotech) on Superfrost Plus

microscope slides (Fisher Scientific). Detailed methods for tissue processing and treatments are included in *SI Appendix, SI Materials and Methods*.

Primary antibodies were diluted in blocking buffer as listed: chicken GFP antibody (GFP-1020, Aves Labs) at 1:1,000, mouse MCM2 antibody (610701, BD Biosciences) at 1:500, rabbit Sox2 antibody (ab97959, Abcam) at 1:500, goat GFAP antibody (ab53554, Abcam) at 1:1,000, rabbit NeuN antibody (12943, Cell Signaling Technology) at 1:1,000, guinea pig DCX antibody (AB2253, MilliporeSigma) at 1:1,000, and mouse BrdU antibody (B35128, ThermoFisher) at 1:500.

Secondary antibodies were diluted in blocking buffer at 1:1,000 as listed: donkey anti-mouse Alexa Fluor 488 (A21202, ThermoFisher Scientific), donkey anti-chicken Cy3 (703-165-155, Jackson ImmunoResearch Laboratories, Inc.), donkey anti-rabbit Alexa Fluor-594 (711-585-152, Jackson ImmunoResearch Laboratories, Inc.), donkey anti-rabbit Alexa Fluor-647 (A31573, ThermoFisher Scientific), donkey anti-goat Alexa Fluor Plus 647 (A32849, ThermoFisher Scientific), and donkey anti-guinea pig Alex Flour-647 (706-605-148, Jackson ImmunoResearch Laboratories, Inc.).

Microscopy and Sampling. One of every 10 sections in a series spanning the entire dentate gyrus was imaged on a confocal microscope (Leica Sp8) using a 40× or 63× Harmonic Compound Plan Apochromat oil Confocal Scanning 2 objective. For lineage analysis, a z-stack of five 3-μm steps was collected per dentate gyrus section for one hemisphere. The dorsal dentate gyrus was quantified, given that Cre expression was variable in the ventral dentate gyrus (77). The upper third of the dentate granule cell layer was defined as being within two dentate granule cell layers of the molecular layer. For behavioral analysis, two sections from both hemispheres were quantified. Images were processed and analyzed using Fiji (ImageJ, NIH). Experimenters were blinded to the genotype of the mice during analysis.

Behavioral Tests. We did not observe overt differences in health between the two genotypes. Mice used for these experiments were healthy, without injuries that would interfere with behavioral testing. Behavioral data were obtained with the help of the Gladstone Behavioral Core. The experimenters were blinded to the genotype of the mice for all behavioral testing.

For behavior experiments, a cohort of adult ∼4-mo-old (age range 13 wk to 17 wk) mice were injected with tamoxifen once per day for five consecutive days. Five weeks after the last tamoxifen injection, behavioral testing began with the elevated plus maze, followed by the open field. Contextual conditioning and discrimination testing began at ∼6.5 wk post tamoxifen injection. Afterward, at ∼10.5 wk post tamoxifen injection, the hot plate test was conducted. Finally, mice were perfused at ∼17.5 wk post tamoxifen injection. Detailed methods for elevated plus maze, open field, contextual fear conditioning and discrimination, and hot plate behavioral tests are included in *SI Appendix, SI Materials and Methods*.

Statistical Analyses. All data were summarized as mean ± SEM. Comparisons between two genotypes were analyzed by unpaired two-tailed Student's *t* tests. If the data did not meet the Student's *t* test's assumptions of normality and variance, the data were analyzed using the unpaired two-tailed Student's *t* test with Welch's correction or the nonparametric Mann–Whitney *U* test, as indicated in the figure legends. Multiple group comparisons were assessed using one-way ANOVA with Holm–Sidak correction for multiple comparisons, two-way ANOVA followed by Sidak's multiple comparisons test, or linear mixed-model with restricted maximum likelihood (REML) and Geisser–Greenhouse correction followed by Sidak's multiple comparisons test, as indicated in the figure legends. The null hypothesis was rejected at $P > 0.05$. Data were analyzed using Prism 9 (GraphPad).

Data Availability. All study data are included in the article and/or *SI Appendix*.

ACKNOWLEDGMENTS. We thank Jeanne Paz, Mazen Kheirbek, John Rubenstein, Mario Zubia, Adeline Yong, and all members of the Y.-N.J. and L.Y.J. laboratories for helpful discussions. We also recognize Marena Tynan-La Fontaine for technical support with mouse experiments; Hirofumi Noguchi for expert technical advice; and members of the Gladstone Behavioral Core, Michael Gill and Iris Lo, for assistance in behavioral experiments. We are grateful to Mazen Kheirbek, Liqun Luo, and David Julius for providing reagents and resources. This work was supported by NSF Graduate Research Fellowships (Grant 1650113 to Y.-H.L.K.; Grant 1650113 to J.V.L.K.), NIH (Grant R01MH065334 to L.Y.J.; Grants NS100954 and NS099188 to E.G.), the Ministry of Science and Technology, Taiwan (Grants 106-2320-B-001-013, 107-2320-B-001-026-MY3, and 110-2314-B-001-007 to S.-B.Y.), and a University of California, San Francisco Chuan-Lyu Discovery Fellowship (J.V.L.K.). Y.-N.J. and L.Y.J. are Howard Hughes Medical Institute Investigators.

Author affiliations: [a]Neuroscience Graduate Program, University of California, San Francisco, CA 94143; [b]Department of Physiology, University of California, San Francisco, CA 94143; [c]Department of Biochemistry and Biophysics, University of California, San Francisco, CA 94143; [d]HHMI, University of California, San Francisco, CA 94143; [e]Behavioral Core, Gladstone Institute of Neurological Disease, Gladstone Institutes, San Francisco, CA 94158; [f]Department of Biological Sciences, Southern Methodist University, Dallas, TX 75275; [g]Institute of Biomedical Sciences, Academia Sinica, Taipei, 115, Taiwan; and [h]Neuroscience Program of Academia Sinica, Academia Sinica, Taipei, 115, Taiwan

1. J. T. Gonçalves, S. T. Schafer, F. H. Gage, Adult neurogenesis in the hippocampus: From stem cells to behavior. *Cell* **167**, 897–914 (2016).
2. J. B. Aimone *et al.*, Regulation and function of adult neurogenesis: From genes to cognition. *Physiol. Rev.* **94**, 991–1026 (2014).
3. C. Anacker, R. Hen, Adult hippocampal neurogenesis and cognitive flexibility - Linking memory and mood. *Nat. Rev. Neurosci.* **18**, 335–346 (2017).
4. G. L. Ming, H. Song, Adult neurogenesis in the mammalian brain: Significant answers and significant questions. *Neuron* **70**, 687–702 (2011).
5. A. Sahay, R. Hen, Adult hippocampal neurogenesis in depression. *Nat. Neurosci.* **10**, 1110–1115 (2007).
6. T. Toda, S. L. Parylak, S. B. Linker, F. H. Gage, The role of adult hippocampal neurogenesis in brain health and disease. *Mol. Psychiatry* **24**, 67–87 (2019).
7. A. M. Bond, G. L. Ming, H. Song, Adult mammalian neural stem cells and neurogenesis: Five decades later. *Cell Stem Cell* **17**, 385–395 (2015).
8. A. Kriegstein, A. Alvarez-Buylla, The glial nature of embryonic and adult neural stem cells. *Annu. Rev. Neurosci.* **32**, 149–184 (2009).
9. K. A. McLaughlin, M. Levin, Bioelectric signaling in regeneration: Mechanisms of ionic controls of growth and form. *Dev. Biol.* **433**, 177–189 (2018).
10. E. Bates, Ion channels in development and cancer. *Annu. Rev. Cell Dev. Biol.* **31**, 231–247 (2015).
11. R. S. Smith, C. A. Walsh, Ion channel functions in early brain development. *Trends Neurosci.* **43**, 103–114 (2020).
12. S. M. Chou *et al.*, K_v1.1 channels regulate early postnatal neurogenesis in mouse hippocampus via the TrkB signaling pathway. *eLife* **10**, e58779 (2021).
13. H. Bao *et al.*, Long-range GABAergic inputs regulate neural stem cell quiescence and control adult hippocampal neurogenesis. *Cell Stem Cell* **21**, 604–617.e5 (2017).
14. R. Rozental *et al.*, Changes in the properties of gap junctions during neuronal differentiation of hippocampal progenitor cells. *J. Neurosci.* **18**, 1753–1762 (1998).
15. J. Song *et al.*, Neuronal circuitry mechanism regulating adult quiescent neural stem-cell fate decision. *Nature* **489**, 150–154 (2012).
16. Y. Tozuka, S. Fukuda, T. Namba, T. Seki, T. Hisatsune, GABAergic excitation promotes neuronal differentiation in adult hippocampal progenitor cells. *Neuron* **47**, 803–815 (2005).
17. T. Yasuda, P. F. Bartlett, D. J. Adams, K_{ir} and K_v channels regulate electrical properties and proliferation of adult neural precursor cells. *Mol. Cell. Neurosci.* **37**, 284–297 (2008).
18. C. Y. Yeh *et al.*, Mossy cells control adult neural stem cell quiescence and maintenance through a dynamic balance between direct and indirect pathways. *Neuron* **99**, 493–510.e4 (2018).
19. A. Kunze *et al.*, Connexin expression by radial glia-like cells is required for neurogenesis in the adult dentate gyrus. *Proc. Natl. Acad. Sci. U.S.A.* **106**, 11336–11341 (2009).
20. M. S. Espósito *et al.*, Neuronal differentiation in the adult hippocampus recapitulates embryonic development. *J. Neurosci.* **25**, 10074–10086 (2005).
21. S. Ge *et al.*, GABA regulates synaptic integration of newly generated neurons in the adult brain. *Nature* **439**, 589–593 (2006).
22. L. S. Overstreet-Wadiche, A. L. Bensen, G. L. Westbrook, Delayed development of adult-generated granule cells in dentate gyrus. *J. Neurosci.* **26**, 2326–2334 (2006).
23. A. Tashiro, V. M. Sandler, N. Toni, C. Zhao, F. H. Gage, NMDA-receptor-mediated, cell-specific integration of new neurons in adult dentate gyrus. *Nature* **442**, 929–933 (2006).
24. J. L. Hallows, B. L. Tempel, Expression of K_v1.1, a Shaker-like potassium channel, is temporally regulated in embryonic neurons and glia. *J. Neurosci.* **18**, 5682–5691 (1998).
25. L. Y. Jan, Y. N. Jan, Voltage-gated and inwardly rectifying potassium channels. *J. Physiol.* **505**, 267–282 (1997).
26. L. Y. Jan, Y. N. Jan, Voltage-gated potassium channels and the diversity of electrical signalling. *J. Physiol.* **590**, 2591–2599 (2012).
27. M. Almgren *et al.*, Lack of potassium channel induces proliferation and survival causing increased neurogenesis and two-fold hippocampus enlargement. *Hippocampus* **17**, 292–304 (2007).
28. L. R. Donahue, S. A. Cook, K. R. Johnson, R. T. Bronson, M. T. Davisson, Megencephaly: A new mouse mutation on chromosome 6 that causes hypertrophy of the brain. *Mamm. Genome* **7**, 871–876 (1996).
29. A. S. Persson *et al.*, K_v1.1 null mice have enlarged hippocampus and ventral cortex. *BMC Neurosci.* **8**, 10 (2007).
30. S. Petersson *et al.*, Truncation of the *Shaker*-like voltage-gated potassium channel, K_v1.1, causes megencephaly. *Eur. J. Neurosci.* **18**, 3231–3240 (2003).
31. S. L. Smart *et al.*, Deletion of the K_v1.1 potassium channel causes epilepsy in mice. *Neuron* **20**, 809–819 (1998).

32. S. B. Yang *et al.*, K_v1.1-dependent control of hippocampal neuron number as revealed by mosaic analysis with double markers. *J. Physiol.* **590**, 2645–2658 (2012).
33. J. S. Espinosa, J. S. Tea, L. Luo, Mosaic analysis with double markers (MADM) in mice. *Cold Spring Harb. Protoc.* **2014**, 182–189 (2014).
34. M. D. Muzumdar, L. Luo, H. Zong, Modeling sporadic loss of heterozygosity in mice by using mosaic analysis with double markers (MADM). *Proc. Natl. Acad. Sci. U.S.A.* **104**, 4495–4500 (2007).
35. H. Zong, J. S. Espinosa, H. H. Su, M. D. Muzumdar, L. Luo, Mosaic analysis with double markers in mice. *Cell* **121**, 479–492 (2005).
36. M. Almgren, M. Schalling, C. Lavebratt, Idiopathic megalencephaly-possible cause and treatment opportunities: From patient to lab. *Eur. J. Paediatr. Neurol.* **12**, 438–445 (2008).
37. J. K. Holth *et al.*, Tau loss attenuates neuronal network hyperexcitability in mouse and *Drosophila* genetic models of epilepsy. *J. Neurosci.* **33**, 1651–1659 (2013).
38. N. B. Danielson *et al.*, Distinct contribution of adult-born hippocampal granule cells to context encoding. *Neuron* **90**, 101–112 (2016).
39. A. Dranovsky *et al.*, Experience dictates stem cell fate in the adult hippocampus. *Neuron* **70**, 908–923 (2011).
40. A. Sahay *et al.*, Increasing adult hippocampal neurogenesis is sufficient to improve pattern separation. *Nature* **472**, 466–470 (2011).
41. K. Trosclair, H. A. Dhaibar, N. M. Gautier, V. Mishra, E. Glasscock, Neuron-specific K_v1.1 deficiency is sufficient to cause epilepsy, premature death, and cardiorespiratory dysregulation. *Neurobiol. Dis.* **137**, 104759 (2020).
42. J. M. Gee *et al.*, Imaging activity in neurons and glia with a *Polr2a*-based and cre-dependent GCaMP5G-IRES-tdTomato reporter mouse. *Neuron* **83**, 1058–1072 (2014).
43. T. Kerloch, S. Clavreul, A. Goron, D. N. Abrous, E. Pacary, Dentate granule neurons generated during perinatal life display distinct morphological features compared with later-born neurons in the mouse hippocampus. *Cereb. Cortex* **29**, 3527–3539 (2019).
44. N. Urbán, F. Guillemot, Neurogenesis in the embryonic and adult brain: Same regulators, different roles. *Front. Cell. Neurosci.* **8**, 396 (2014).
45. E. Gould, A. Beylin, P. Tanapat, A. Reeves, T. J. Shors, Learning enhances adult neurogenesis in the hippocampal formation. *Nat. Neurosci.* **2**, 260–265 (1999).
46. G. Kempermann, H. G. Kuhn, F. H. Gage, More hippocampal neurons in adult mice living in an enriched environment. *Nature* **386**, 493–495 (1997).
47. H. G. Kuhn, C. M. Cooper-Kuhn, Bromodeoxyuridine and the detection of neurogenesis. *Curr. Pharm. Biotechnol.* **8**, 127–131 (2007).
48. J. M. Wojtowicz, N. Kee, BrdU assay for neurogenesis in rodents. *Nat. Protoc.* **1**, 1399–1405 (2006).
49. M. A. Bonaguidi *et al.*, In vivo clonal analysis reveals self-renewing and multipotent adult neural stem cell characteristics. *Cell* **145**, 1142–1155 (2011).
50. J. P. Brown *et al.*, Transient expression of doublecortin during adult neurogenesis. *J. Comp. Neurol.* **467**, 1–10 (2003).
51. S. Couillard-Despres *et al.*, Doublecortin expression levels in adult brain reflect neurogenesis. *Eur. J. Neurosci.* **21**, 1–14 (2005).
52. T. Plümpe *et al.*, Variability of doublecortin-associated dendrite maturation in adult hippocampal neurogenesis is independent of the regulation of precursor cell proliferation. *BMC Neurosci.* **7**, 77 (2006).
53. G. Kempermann, D. Gast, G. Kronenberg, M. Yamaguchi, F. H. Gage, Early determination and long-term persistence of adult-generated new neurons in the hippocampus of mice. *Development* **130**, 391–399 (2003).
54. X. Duan *et al.*, Disrupted-in-schizophrenia 1 regulates integration of newly generated neurons in the adult brain. *Cell* **130**, 1146–1158 (2007).
55. S. Ibrahim *et al.*, Traumatic brain injury causes aberrant migration of adult-born neurons in the hippocampus. *Sci. Rep.* **6**, 21793 (2016).
56. J. Terreros-Roncal *et al.*, Activity-dependent reconnection of adult-born dentate granule cells in a mouse model of frontotemporal dementia. *J. Neurosci.* **39**, 5794–5815 (2019).
57. S. P. Cahill, R. Q. Yu, D. Green, E. V. Todorova, J. S. Snyder, Early survival and delayed death of developmentally-born dentate gyrus neurons. *Hippocampus* **27**, 1155–1167 (2017).
58. T. Ciric, S. P. Cahill, J. S. Snyder, Dentate gyrus neurons that are born at the peak of development, but not before or after, die in adulthood. *Brain Behav.* **9**, e01435 (2019).
59. A. G. Dayer, A. A. Ford, K. M. Cleaver, M. Yassaee, H. A. Cameron, Short-term and long-term survival of new neurons in the rat dentate gyrus. *J. Comp. Neurol.* **460**, 563–572 (2003).
60. C. A. Denny, N. S. Burghardt, D. M. Schachter, R. Hen, M. R. Drew, 4- to 6-week-old adult-born hippocampal neurons influence novelty-evoked exploration and contextual fear conditioning. *Hippocampus* **22**, 1188–1201 (2012).
61. C. A. Denny *et al.*, Hippocampal memory traces are differentially modulated by experience, time, and adult neurogenesis. *Neuron* **83**, 189–201 (2014).
62. M. R. Drew, C. A. Denny, R. Hen, Arrest of adult hippocampal neurogenesis in mice impairs single- but not multiple-trial contextual fear conditioning. *Behav. Neurosci.* **124**, 446–454 (2010).
63. M. D. Saxe *et al.*, Ablation of hippocampal neurogenesis impairs contextual fear conditioning and synaptic plasticity in the dentate gyrus. *Proc. Natl. Acad. Sci. U.S.A.* **103**, 17501–17506 (2006).
64. T. Nakashiba *et al.*, Young dentate granule cells mediate pattern separation, whereas old granule cells facilitate pattern completion. *Cell* **149**, 188–201 (2012).
65. S. Tronel *et al.*, Adult-born neurons are necessary for extended contextual discrimination. *Hippocampus* **22**, 292–298 (2012).
66. N. M. Ben Abdallah, L. Slomianka, A. L. Vyssotski, H. P. Lipp, Early age-related changes in adult hippocampal neurogenesis in C57 mice. *Neurobiol. Aging* **31**, 151–161 (2010).
67. T. E. Tracy *et al.*, Acetylated tau obstructs KIBRA-mediated signaling in synaptic plasticity and promotes tauopathy-related memory loss. *Neuron* **90**, 245–260 (2016).
68. B. J. Piggott *et al.*, Paralytic, the *Drosophila* voltage-gated sodium channel, regulates proliferation of neural progenitors. *Genes Dev.* **33**, 1739–1750 (2019).
69. R. S. Smith *et al.*, Sodium channel *SCN3A* (Na_v1.3) regulation of human cerebral cortical folding and oral motor development. *Neuron* **99**, 905–913.e7 (2018).
70. I. Vitali *et al.*, Progenitor hyperpolarization regulates the sequential generation of neuronal subtypes in the developing neocortex. *Cell* **174**, 1264–1276.e15 (2018).
71. N. Urbán, I. M. Blomfield, F. Guillemot, Quiescence of adult mammalian neural stem cells: A highly regulated rest. *Neuron* **104**, 834–848 (2019).
72. S. Bottes *et al.*, Long-term self-renewing stem cells in the adult mouse hippocampus identified by intravital imaging. *Nat. Neurosci.* **24**, 225–233 (2021).
73. G. A. Pilz *et al.*, Live imaging of neurogenesis in the adult mouse hippocampus. *Science* **359**, 658–662 (2018).
74. J. Terreros-Roncal *et al.*, Impact of neurodegenerative diseases on human adult hippocampal neurogenesis. *Science* **374**, 1106–1113 (2021).
75. F. Tronche *et al.*, Disruption of the glucocorticoid receptor gene in the nervous system results in reduced anxiety. *Nat. Genet.* **23**, 99–103 (1999).
76. B. Tasic *et al.*, Extensions of MADM (mosaic analysis with double markers) in mice. *PLoS One* **7**, e33332 (2012).
77. S. Jinno, Topographic differences in adult neurogenesis in the mouse hippocampus: A stereology-based study using endogenous markers. *Hippocampus* **21**, 467–480 (2011).